EBioMedicine 50 (2019) 355–365

Contents lists available at ScienceDirect

EBioMedicine

journal homepage: www.elsevier.com/locate/ebiom

Research paper

Radiomics analysis of placenta on T2WI facilitates prediction of postpartum haemorrhage: A multicentre study

Qingxia Wu[a,1], Kuan Yao[b,c,1], Zhenyu Liu[c,d,1], Longfei Li[c,e], Xin Zhao[f], Shuo Wang[c,g], Honglei Shang[f], Yusong Lin[e], Zejun Wen[f,*], Jie Tian[c,d,g,h,*], Meiyun Wang[a,*]

[a] Department of Medical Imaging, Henan Key Laboratory of Neurological Imaging, Henan Provincial People's Hospital, People's Hospital of Zhengzhou University, People's Hospital of Henan University, Zhengzhou, Henan, China
[b] School of Biomedical Engineering, Shanghai Jiao Tong University, Shanghai, China
[c] CAS Key Laboratory of Molecular Imaging, Institute of Automation, Chinese Academy of Sciences, Beijing, China
[d] University of Chinese Academy of Sciences, Beijing, China
[e] Collaborative Innovation Centre for Internet Healthcare, Zhengzhou University, Zhengzhou, Henan, China
[f] Department of Radiology, the Third affiliated Hospital of Zhengzhou University, Zhengzhou, Henan, China
[g] Beijing Advanced Innovation Centre for Big Data-Based Precision Medicine, School of Medicine, Beihang University, Beijing, China
[h] Engineering Research Centre of Molecular and Neuro Imaging of Ministry of Education, School of Life Science and Technology, Xidian University, Xi'an, Shanxi, China

ARTICLE INFO

Article History:
Received 28 August 2019
Revised 4 November 2019
Accepted 7 November 2019
Available online 22 November 2019

Keywords:
Radiomics
Placenta accreta spectrum
Postpartum haemorrhage
Estimated blood loss
Magnetic resonance imaging

ABSTRACT

Background: Identification of pregnancies with postpartum haemorrhage (PPH) antenatally rather than intrapartum would aid delivery planning, facilitate transfusion requirements and decrease maternal complications. MRI has been increasingly used for placenta evaluation. Here, we aim to build a nomogram incorporating both clinical and radiomic features of placenta to predict the risk for PPH in pregnancies during caesarian delivery (CD).

Methods: A total of 298 pregnant women were retrospectively enrolled from Henan Provincial People's Hospital (training cohort: $n = 207$) and from The Third Affiliated Hospital of Zhengzhou University (external validation cohort: $n = 91$). These women were suspected with placenta accreta spectrum (PAS) disorders and underwent MRI for placenta evaluation. All of them underwent CD and were singleton. PPH was defined as more than 1000 mL estimated blood loss (EBL) during CD. Radiomic features were selected based on their correlations with EBL. Radiomic, clinical, radiological, clinicoradiological and clinicoradiomic models were built to predict the risk of PPH for each patient. The model with the best prediction performance was validated with its discrimination ability, calibration curve and clinical application.

Findings: Thirty-five radiomic features showed strong correlation with EBL. The clinicoradiomic model resulted in the best discrimination ability for risk prediction of PPH, with AUC of 0.888 (95% CI, 0.844–0.933) and 0.832 (95% CI, 0.746–0.913), sensitivity of 91.2% (95% CI, 85.8%-96.7%) and 97.6% (95% CI, 92.7%-100%) in the training and validation cohort respectively. For patients with severe PPH (EBL more than 2000 mL), 53 out of 55 pregnancies (96.4%) in the training cohort and 18 out of 18 (100%) pregnancies in the validation cohort were identified by the clinicoradiomic model. The model performed better in patients without placenta previa (PP) than in patients with PP, with AUC of 0.983 compared with 0.867, sensitivity of 100% compared with 90.8% in the training cohort, AUC of 0.832 compared with 0.815, sensitivity of 97.6% compared with 97.2% in the validation cohort.

Interpretation: The clinicoradiomic model incorporating both prenatal clinical factors and radiomic signature of placenta on T2WI showed good performance for risk prediction of PPH. The predictive model can identify severe PPH with high sensitivity and can be applied in patients with and without PP.

Abbreviations: PPH, Postpartum Haemorrhage; EBL, Estimated Blood Loss; CD, Cesarean Delivery; PAS, Placenta Accreta Spectrum; MRI, Magnetic resonance imaging; PACS, Picture Archiving and Communication system; SSFSE, Single Shot Fast Spin Echo; HASTE, Half-Fourier Acquisition Single-shot Turbo spin Echo; T2WI, T2-Weighted Imaging; PP, Placenta Previa; VOI, Volume of Interest; LASSO, Least Absolute Shrinkage and Selection Operator; SVM, Support Vector Machine; AIC, Akaike's Information Criterion; NRI, Net Reclassification Improvement; IDI, Integrated Discrimination Improvement

* Corresponding authors.
E-mail addresses: zxa@vip.163.com (Z. Wen), jie.tian@ia.ac.cn (J. Tian), mywang@ha.edu.cn (M. Wang).
[1] These authors contributed equally to this article.

https://doi.org/10.1016/j.ebiom.2019.11.010

Research in context

Evidence before this study

Magnetic resonance imaging (MRI) has been increasingly used for placenta estimation and provides more comprehensive evaluation compared with ultrasound. Previous studies have built predictive models either for postpartum haemorrhage (PPH) or hysterectomy or blood transfusion prediction in pregnancies based on clinical factors and ultrasound findings. However, the evaluation of ultrasound features of placenta depends on the experiences of doctors and varies among institutions. We searched PubMed and Web of Science, for research articles with the following terms: "(postpartum haemorrhage OR postpartum bleeding OR estimated blood loss OR blood loss OR transfusion OR hysterectomy OR uterine artery embolism) AND (placenta OR placenta accreta OR placenta increta OR placenta percreta OR placenta accreta spectrum OR PAS) AND (signature OR model) AND (radiomic OR texture) AND (magnetic resonance imaging OR MRI)". This search did not identify any previous radiomic model for PPH prediction in pregnancies who underwent placental MRI.

Added value of this study

To our knowledge, this is the first study to build a clinicoradiomic model based on the radiomic features of placenta on T2WI and clinical factors to predict the risk for PPH in pregnancies suspected with placenta accreta spectrum (PAS) disorders. The radiomic features of placenta on T2WI showed strong correlation with estimated blood loss (EBL). The clinicoradiomic model we built incorporating 35 radiomic features of placenta and 3 clinical factors can identify more than 91% of pregnancies with PPH. Fifty three out of 55, 18 out of 18 patients with severe PPH (EBL more than 2000 mL) were identified in the training and validation cohorts respectively. The good performance of the clinicoradiomic model in subgroups with and without PP suggested that the clinicoradiomic model can be applied for all patients suspected with PAS disorders who underwent MRI.

Implications of all the available evidence

Our findings suggest that the clinicoradiomic model can be applied in routine clinical use for PPH prediction in pregnant women suspected with PAS disorders who underwent MRI examination.

1. Introduction

Postpartum haemorrhage (PPH) is one of the leading causes of maternal complications and mortality worldwide, which is usually defined as more than 1000 mL estimated blood loss (EBL) for cesarean delivery (CD) [1,2]. Early identification of patients with PPH, predicting the need for blood products antenatally rather than intrapartum would aid delivery planning, facilitate the preparation of blood products and transfusion requirements, as well as decrease maternal complications [3,4]. With the increase of maternal age and the number of abortion and CD, the incidence of placenta accreta spectrum (PAS) disorders is rising and is now estimated to be 1 in 500 to 1 in 300 pregnancies [5,6]. PAS disorders, accompanied by incomplete separation of placenta and insufficient uterine contraction, often result in massive hemorrhage during delivery [7].

Ultrasound is the primary tool for PAS disorders diagnosis [8]. Magnetic resonance imaging (MRI) usually serves as an important adjuvant tool to ultrasound. Until now, most studies of MRI concentrated on the antenatal diagnostic accuracy of PAS disorders and several meta-analyses concluded that diagnostic accuracy of PAS disorders was statistically similar to ultrasound alone [9–11]. This did not provide additional value for clinicians and surgeons when an ultrasound has already been performed [12]. The purpose of MRI for possible PAS patients suspected by ultrasound should be to provide additional helpful information such as the extent and degree of placental invasion, the presence of extrauterine involvement and to predict the emergency situation during the operation process (such as blood loss, transfusion and hysterectomy) and thus help to improve the care of patients with PAS disorders in higher-level medical centers. However, with the increase of gestational weeks, myometrial thinning and placental signal heterogeneity, the signs indicating PAS disorders on MRI become harder to evaluate and more dependent on the experience of radiologists [13].

Radiomics analysis quantifying high-dimensional tissue features that cannot be observed by the naked eye has shown great potential in precision medicine, most of which were in the oncological field [14–16]. Radiomics analysis provides us a quantitative method to reflect tissue or tumor heterogeneity and tends to be more stable compared with subjective evaluation. The studies of radiomics analysis for placenta evaluation have emerged recently but until now are relatively rare [17–20]. These studies found texture analysis of placenta is a feasible tool for PAS diagnosis and even PAS severity assessment [18]. Siauve N stated that radiomics analysis or machine learning is especially suitable for placenta evaluation with increased heterogeneity in late gestational weeks [17]. However, all the above studies were limited with relatively small sample size and lack of external validation dataset.

To the best of our knowledge, until now there is no reported study predicting PPH or EBL during CD based on the radiomic or texture features of placenta in patients suspected with PAS disorders. Therefore, the aim of our study is first, to extract the radiomic features of placenta which are highly correlated with EBL, and at the same time, stable among multiple centres, and second, to establish a nomogram to facilitate the prediction of PPH in women undergoing CD.

2. Materials and methods

2.1. Study population

The study was approved by the ethics committee of Henan Provincial People's Hospital and The Third affiliated Hospital of Zhengzhou University. Informed consent from patients were waived for this retrospective study. From May 2013 to April 2019, pregnant women who underwent placental MRI were retrospectively collected from the picture archiving and communication system (PACS) in Henan Provincial People's Hospital (Zhengzhou, China) and The Third affiliated Hospital of Zhengzhou University (Zhengzhou, China). The inclusion criteria were: (a), all singleton pregnancies suspected with PAS disorders who underwent MRI for placenta evaluation; (b), all patients who underwent CD; (c), EBL and transfusion protocol were available. The exclusion criteria were: (a), pregnancy terminated by uterine curettage or induced 1abor; (b), retained placental tissue after induced 1abor or birth; (c), not giving birth at one of the two hospitals; (d), patients with poor image quality or severe motion artifacts or missing images; (e), patients with vaginal delivery.

Finally, considering the larger sample size, 207 patients from Henan Provincial People's Hospital were enrolled as the training cohort, and 91 patients from The Third affiliated Hospital of Zhengzhou University were enrolled as the validation cohort. The patient recruitment flowchart was shown in Fig. S1.

Patients' characteristics including maternal age, gravidity, parturition, abortion, previous cesarean deliveries, vaginal bleeding during pregnancy, gestational age at MRI and delivery, pregnancy complications such as hypertension and diabetes, placenta position and presence of PAS evaluated by ultrasound and hemoglobin value before CD were extracted from the medical records. The definition of

placenta position and the image features indicating PAS diagnosis on ultrasound were shown in Supplementary Methods.

All patients underwent CD. Surgical procedures like elective or emergency CD, hemostasis techniques during operation including intrauterine tamponade or packing, lifting suture of cervical or lower uterine, B-lynch sutures, wedge resection of uterus, abdominal aortic balloon implantation, uterine artery embolism, uterine artery ligation or suture, hysterectomy and any other surgeries were recorded. The EBL during surgery, blood transfusion protocoland postpartum diagnosis of PAS were obtained by reviewing the medical records.

All patients underwent placental MRI using one of the two 3.0T MRI systems, either with (Discovery MR 750; GE Medical Systems, Milwaukee, Wis) or (Skyra; Siemens Healthineers). The image protocols and detailed parameters were shown in Supplementary Methods and Table. S1.

2.2. Radiological evaluation

The flowchart of the study was shown in Fig. 1. Two radiologists (Qingxia Wu and Yan Wang, with 9 and 10 years of pelvic imaging experience respectively) evaluated the image findings separately on a dedicated software (Radiant DICOM Viewer 4.6.9). Both readers were blinded to previous MRI interpretation, each other's interpretation, previous ultrasound reports, and the surgical and pathologic reports from delivery.

Since it is difficult to differentiate the spectrum of placenta accreta, increta and percreta, in this article, PAS refers to all the three conditions unless specially noted. Image features that are highly indicative of abnormal placentation according to published literatures on MRI were assessed in terms of their presence or absence [21,22]. These features were listed in the following order: (1) placenta previa (PP), including complete and partial PP; (2) intraplacental nodular or linear dark bands; (3) focal blurring or interruption of myometrial border; (4) intraplacental abnormal vascularity; (5) uterine bulging with loss of normal shape of the uterus; (6) bladder tenting; and (7) direct visualization of adjacent tissue invasion, usually bladder.

Consensus was made in cases of disagreement after completion of all readings.

2.3. Radiomic feature selection

2.3.1. Image segmentation

Sagittal SSFSE or HASTE T2WI, the optimal position for the uterus and placenta observation, was retrieved from PACS for placenta segmentation. One radiologist with 9 years of pelvic MR imaging experience performed all the segmentations of placental tissue manually with an open-source ITK-SNAP software (www.itksnap.org).

Frequently it is hard to identify the interface between the placenta and myometrium, so both the placental tissue and the underlying myometrium were delineated. Previous studies reported that the cervical length before delivery showed association with massive PPH in pregnancies with PP [23]. A new sonographic jellyfish sign, the absence of the normal linear demarcation between the placenta previa and the cervix, was also reported to correlate with maternal complications [24]. For patients with PP, the cervix was also included in the segmentation, as illustrated in Fig. 2. Each segmentation was validated by a senior radiologist, who had 19 years of experience. The segmented tissues on each slice were fused to generate VOI for radiomic feature evaluation.

2.3.2. Radiomic feature extraction

After manual segmentation, T2WI was standardized using z-score normalization to obtain a standard normal distribution of the image intensities.

Considering the potential of texture features to reflect the heterogeneity of placenta, which increases significantly with gestational week during pregnancy, we paid more attention to texture features. Since the shape of placenta and uterus were indicative of

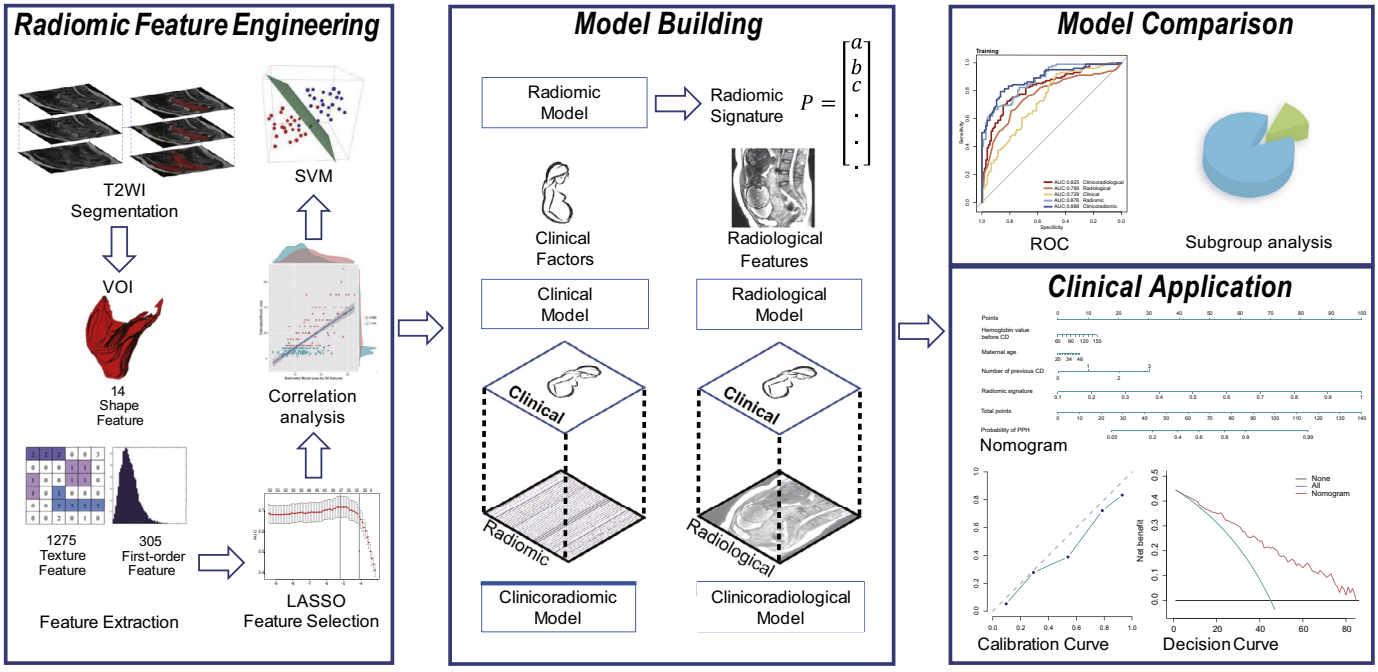

Fig. 1. The flowchart of the study. This study included radiomic feature engineering, model building, model comparison and clinical application. The placental tissues were segmented to generate volume of interest (VOI) and then 1595 quantitative radiomic features were extracted from placenta VOI. The least absolute shrinkage and selection operator (LASSO) was then used to select the features which were highly correlated with EBL. Pearson correlation analysis was conducted to validate the correlation between these features and EBL. Based on the selected features, a radiomic signature was constructed using the Gaussian kernel support vector machine model, which is called radiomic model. Based on clinical factors as well as radiological features, clinical model and radiological model were built respectively. Clinical factors were combined with radiological features and radiomic signature to generate clinicoradiological and clinicoradiomic model. Model comparison was conducted to select the optimal model with best performance for postpartum haemorrhage prediction. Finally, the calibration and decision curve analysis were conducted to validate the performance and clinical value of the optimal model.

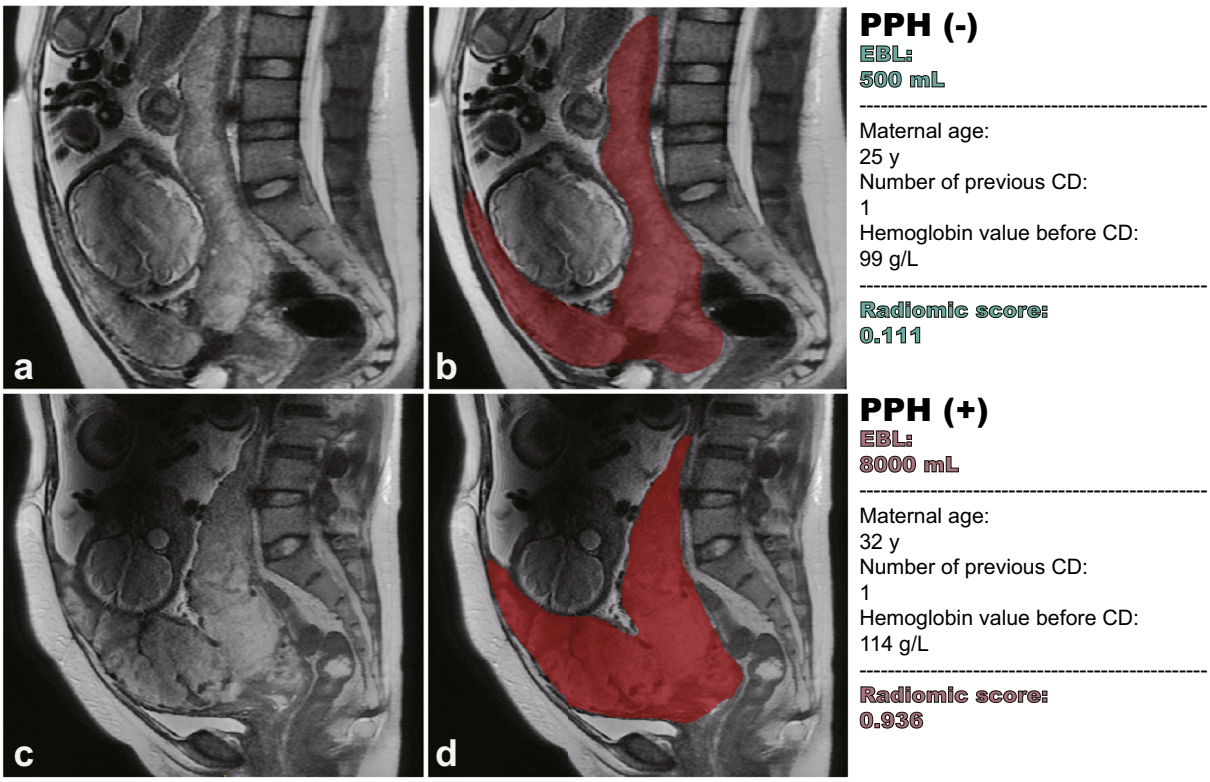

Fig. 2. Representative cases and delineation of placenta. (a, b) A 25-year-old woman at 33+2 gestation weeks with placenta previa. She had a history of G4P2L2A0 with one previous CD. The hemoglobin level was 99 g/L before CD. She had an EBL of 500 mL during CD. Based on the clinicoradiomic model the predicted radiomic score was 0.111 and she was classified as without PPH. (c, d) A 32-year-old woman at 35+6 gestation weeks with placenta previa. She had a history of G3P1L1A1 with one previous CD. The hemoglobin level was 114 g/L before CD. She had an EBL of 8000 mL during CD. Based on the clinicoradiomic model the predicted radiomic score was 0.936 and she was classified as with PPH. Although the two placentas on T2WI showed similar radiological features in the eyes of radiologists, their radiomic scores were significantly different, predicting PPH precisely. Since it was hard to identify the interface between placenta and subplacental myometrium, as shown in (b) and (d), the placental tissue, the underlying myometrium and the cervix were all delineated to generate VOI of placenta.

abnormal placentation, we also evaluated the shape features of the VOI of placenta.

1595 radiomic features were extracted from the placenta VOI using pyradiomic 2.2.0, including i) 14 shape features, ii) 306 first order features, iii) 1275 texture features. The details of radiomic features were listed in Supplementary Methods.

2.3.3. Feature selection and verification

To select the radiomic features highly correlated with EBL during CD, we used least absolute shrinkage and selection operator (LASSO) regression with three-fold cross-validation. Pearson correlation analysis was applied to examine the correlation between the selected features and the EBL. Correlation analysis was also conducted between the selected radiomic features and radiological features to determine whether these features are correlated with each other.

2.4. Model building and radiomic signature validation

As shown in the model building part of Fig. 1, we built 5 models using different combinations of factors. Radiomic, clinical and radiological models were generated from radiomic features, clinical factors and radiological features respectively. Clinicoradiomic model analysed clinical factors and radiomic features jointly while clinicoradiological model included clinical factors as well as the radiological features extracted by radiologists, which represented the model currently used in clinical.

After feature selection, we built the radiomic model using the support vector machine (SVM) algorithm with a radial basis kernel for risk prediction of PPH based on the selected radiomic features. The final regularization parameter was determined by the max AUC in the training cohort with three-fold cross-validation. Thereafter, the radiomic model predicted a radiomic signature indicating the probability of PPH for each sample.

To validate the performance improvement after the inclusion of radiomic signature, the models with radiomic signature (radiomic model, clinicoradiomic model) and the models without radiomic signature (clinical model, radiological model, clinicoradiological model) were compared.

The correlation between prenatal clinical factors, radiological features suggesting PAS evaluated by radiologists and EBL were tested via Spearman correlation analysis, with the p-value set to 0.05. Features with p-value more than 0.05 were excluded from the model. Then multiple regression analysis was employed, backward stepwise selection method with the stopping rule based on Akaike's information criterion (AIC) was conducted for clinical and radiological feature selection, based on which clinical model and radiological model were built.

The performance improvement introduced by the inclusion of radiomic features was quantified by net reclassification improvement (NRI) and integrated discrimination improvement (IDI).

NRI offered a meaningful index of classification accuracy, quantifying the amount of correct reclassified samples introduced by radiomic signature. IDI indicated integrated discrimination improvement [25]. The p-values associated with NRI and IDI indicated whether the improvement of reclassification after the inclusion of radiomic signature was statistically significant.

After model comparison, a nomogram for clinical use was built based on the model with the best discrimination ability of PPH. The performance of the nomogram was evaluated with its discrimination ability, calibration curve and clinical application.

2.6. Statistical analysis

All the statistical analyses in this study were implemented with Python 3.7.1 (https://www.python.org), R software (version 3.4.1; http://www.Rproject.org) and IBM SPSS 22.0 for Windows (IBM Corp, Armonk, New York). Python was used to extract and select the radiomic features as well as build the prediction models. R software was used for evaluating the prediction models. SPSS was used to compare the variables between different cohorts. The logistic regression with LASSO penalty and the SVM model were implemented using Python 3.7.1 in the Scikit-learn package (version 0.21.3). The Kolmogorov-Smirnov test was explored to detect whether the distribution of numeric value was normal. Nonparametric Mann-Whitney U test and Pearson Chi square test were used to explore the difference between the training and validation cohorts. The correlation of clinical and radiological factors with EBL and PPH were analyzed using spearman correlation test. The significance threshold was set at 0.05.

3. Results

3.1. Patient characteristics, EBL and PPH

Prenatal clinical information, EBL and postpartum PAS diagnosis in the training and validation cohorts were shown in Table 1. There was no significant distribution difference when the PPH was categorized as more than 1000 mL EBL between the two cohorts (p=.502). The median EBL were 2000 and 1800 mL for the 102 and 41 patients with PPH in the training and validation cohorts respectively. These two cohorts were similar in their distribution of maternal age, gravidity, previous parturition, abortion and CD. The intrapartum surgical procedures were shown in Table S2. The correlation coefficient between EBL and final diagnosis of PAS after surgery was 0.404 (p<.001), whereas there was no correlation with EBL and final diagnosis of PAS in the validation cohort (p=.171).

3.2. Radiomic features correlated with EBL

In total, 1595 radiomic features were extracted from each VOI of the placenta on T2WI. Among them, 35 features were selected using the LASSO logistic regression algorithm. The 35 radiomic features can be seen in Table S3. The correlation analysis between these 35 radiomic features and 7 radiological features can be seen in Fig. 3.

Since most of the selected features (34/35) were extracted from the filter-filtered images and over half of them were obtained by wavelet transform, texture features and high dimensional features were more relevant with EBL. These features extracted by algorithms also showed consistency with some radiological features extracted by radiologists (Fig. 3). For example, intraplacental abnormal vascularity was correlated with wavelet-HLL_firstorder_Energy feature and wavelet-HLL_firstorder_TotalEnergy feature both in training and validation cohort (p<.05). The correlation between these features demonstrated that although some texture features were high

Table 1
Patient clinical characteristics in the training and validation cohorts.

Characteristics	Training Cohort n = 207			Validation Cohort n = 91			P
	PPH (+) n = 102	PPH (-) n = 105	p	PPH (+) n = 41	PPH (-) n = 50	p	
Maternal Age, years (Median, range)	31.5,23–46	31,20–44	.180	33,24–47	32,20–44	.257	.232
Gravidity (Median, range)	4,1–9	3,1–7	.001	3,2–6	3,1–12	.019	.171
Parturition (Median, range)	1,0–3	1,0–3	.000	1,0–3	1,0–2	.033	.636
Abortion (Median, range)	1,0–5	1,0–4	.024	1,0–4	1,0–9	.162	.393
Previous CD (Median, range)	1,0–3	1,0–3	.000	1,0–3	1,0–2	.000	.772
Hemoglobin value before CD (g/L) Mean, range	101,65–134	105,81–135	.028	107,63–143	109,68–134	.578	.005
Vaginal bleeding during pregnancy			.081			.185	.008
Yes	43	57		16	13		
No	59	48		25	37		
Gestational age at MRI, weeks			.689			.595	.000
<30	7	7		6	4		
≥30, <34	34	41		5	6		
≥34	61	57		30	40		
Gestational age at delivery			.409			.875	0.000
Full term	24	30		19	24		
Preterm	78	75		22	26		
Pregnancy complications			.170			1.000	.247
Negative	88	83		36	44		
Positive	14	22		5	6		
Ultrasound placenta previa			.034			.007	.100
Negative	19	33		2	13		
Positive	83	72		39	37		
Ultrasound PAS status			.000			.000	.005
Negative	62	88		14	37		
Positive	40	17		27	13		
CD			.411			.290	.636
Elective	92	98		35	47		
Emergency	10	7		6	3		
Estimated blood loss, mL (Median, range)	2000,1000–8000	600, 200–900	.000	1800,1000–5000	500,200–950	.000	.055
Blood transfusion			.000			.000	.005
Yes	100	69		37	10		
No	2	36		4	40		
Final diagnosis of PAS			.000			.499	.420
Negative	2	27		0	2		
Positive	100	78		41	48		

Abbreviations: PPH: Postpartum Haemorrhage; CD: Caesarian Delivery; PAS: Placenta accreta spectrum.

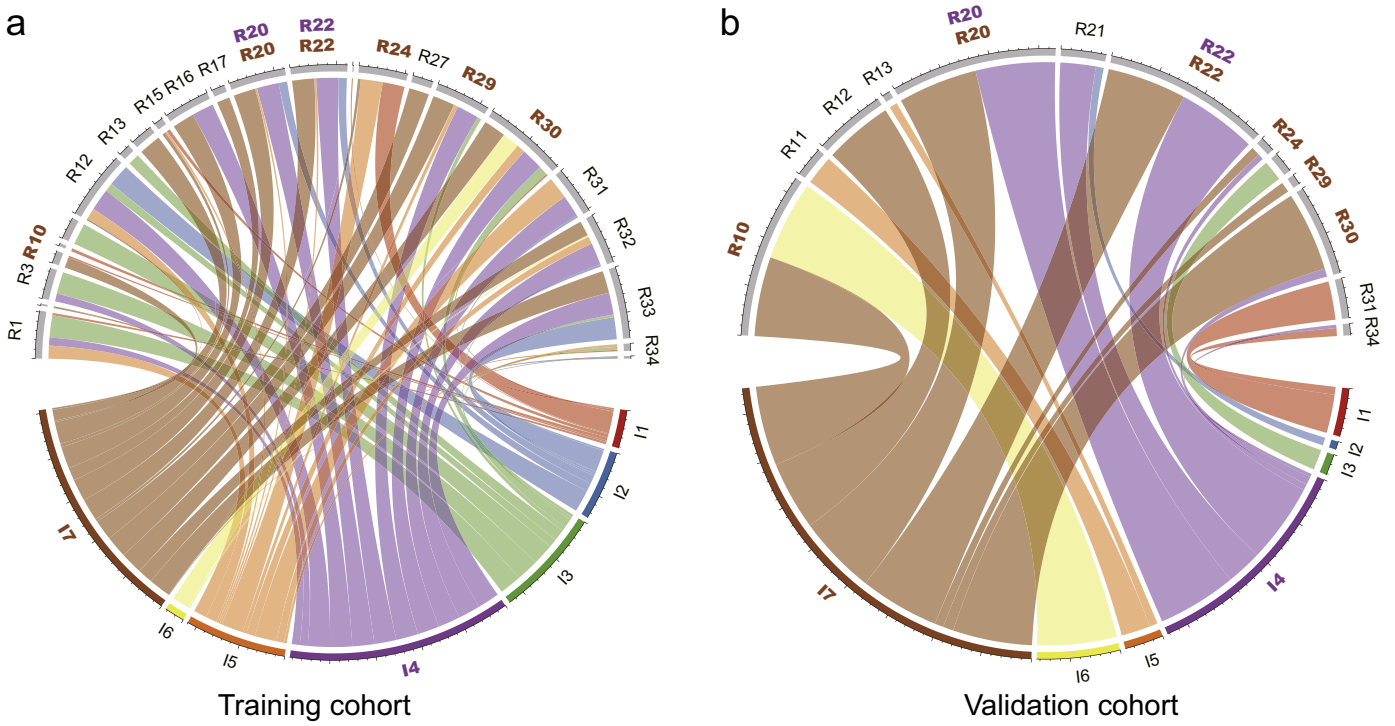

Fig. 3. Chord diagram of the correlation between 35 radiomic features and 7 radiological features. Correlation analysis of selected radiomic features and radiological features in training (a) and validation (b) cohorts. Each link represented one correlation that was significant with the p-value<0.05 by Pearson correlation analysis. Width of links were proportional to the strength of the correlation. R1–R35 represented the selected radiomic features in order (Table S3) and I1 – I7 represented 7 radiological features in order which can be seen in MRI features from radiological evaluation, which were highlighted using color brown. I7 (direct visualization of adjacent tissues invasion) was found highly correlated with R20, R22, R24, R29 and R30 both in training and validation cohorts. I4 (intraplacental abnormal vascularity) was found highly correlated with R20 and R24 both in training and validation cohorts, which were highlighted using color purple. (For interpretation of the references to color in this figure legend, the reader is referred to the web version of this article.)

dimensional features which could not be observed by the naked eye, several specific combinations of these features can be explained by some radiological features to some extent.

As shown in Fig. 4a and b, the blood loss predicted by 35 features were highly correlated with the EBL. The Pearson correlation coefficients of training and validation cohorts were 0.682 ($p<$ .0001) and 0.353 (p=.0006).

Thereafter, a radiomic signature was constructed using the Gaussian kernel SVM. The AUC and classification sensitivity of radiomic signature from the training cohort were 0.876 (95% CI, 0.832–0.820) and 89.2% (95% CI, 83.2–95.3%), from the validation cohort were 0.795 (95% CI, 0.705–0.885) and 92.7% (95% CI, 84.8–100%) (Fig. 4c and d).

The distribution of radiomic signature and PPH of the individual were presented in Fig. 4e and f, which clearly reveals that almost all patients with PPH (92.7%, 38/41) would avoid being misclassified by using the cutoff value of the radiomic signature.

3.3. Model building and radiomic signature validation

For prenatal clinical factors, Spearman correlation analysis showed that maternal age, gravidity, parturition, abortion, previous CD, hemoglobin value before CD and vaginal bleeding during pregnancy significantly correlated with EBL in the training cohort, with p value of 0.008, <0.0001, <0.0001, 0.034, <0.0001, 0.008 and 0.031 respectively (Table S4). After AIC analysis, maternal age, number of previous CD and hemoglobin value before CD were enrolled in the clinical model.

There was a significant difference for the MRI features suggesting PAS between training and validation cohort, as shown in Table S5. All the seven image features suggesting PAS showed statistical correlation with EBL in the training cohort. They were all enrolled to build radiological model.

The clinicoradiomic model, developed by incorporating radiomic signature with clinical factors (Fig. 5), resulted in an AUC of 0.888 (95% CI, 0.844–0.933) and 0.832 (95% CI, 0.746–0.913) for PPH prediction in the training and validation cohort respectively. The performance of radiomic signature, clinical, radiological, clinicoradiological and clinicoradiomic models were shown in Table 2 and Fig. 5.

The clinicoradiomic model showed the best discrimination ability, with the sensitivity of 91.2% (95% CI, 85.8%–96.7%) and 97.6% (95% CI, 92.7%–100%) in the training and validation cohort respectively. The calculation formula of clinicoradiomic model was listed in Supplementary results.

Subgroup analysis was also conducted to validate the performance of the clinicoradiomic model. For patients with severe PPH, here defined as more than 2000 mL EBL, 53 out of 55 (96.4%), 18 out of 18 (100%) pregnancies were identified by the clinicoradiomic model. For pregnancies with and without PP, the performance of clinicoradiomic model for PPH prediction was shown in Table 3. Clinicoradiomic model performed better in patients without PP than that with PP, with AUC of 0.983 (95%CI, 0.949–1.000) versus 0.867 (95%CI, 0.813–0.921), sensitivity of 100% (95%CI, 100%–100%) versus 90.8% (95%CI, 84.8%–96.7%) in the training cohort and AUC of 0.832 (95%CI, 0.748–0.912) versus 0.815 (95%CI, 0.718–0.913), sensitivity of 97.6% (95%CI, 92.8%–100%) versus 97.2% (95%CI, 91.9%–100%) in the validation cohort.

The NRI and IDI of clinicoradiomic model versus clinical model from the training cohort were 0.899 ($p<$.0001) and 0.298 (95%CI, 0.235–0.361, $p<$.0001), from the validation cohort were 0.801 ($p<$.0001) and 0.192 (95%CI, 0.093–0.290, p=.00015), respectively, which highlighted the performance improvement introduced by radiomic signature. The introduction of clinical factors also benefited the prediction of PPH. When compared with the radiomic model, the clinicoradiomic model showed improvement in integrated discrimination with an IDI of 0.064 (95%CI, 0.027–0.102, p=.00075) in the validation cohort.

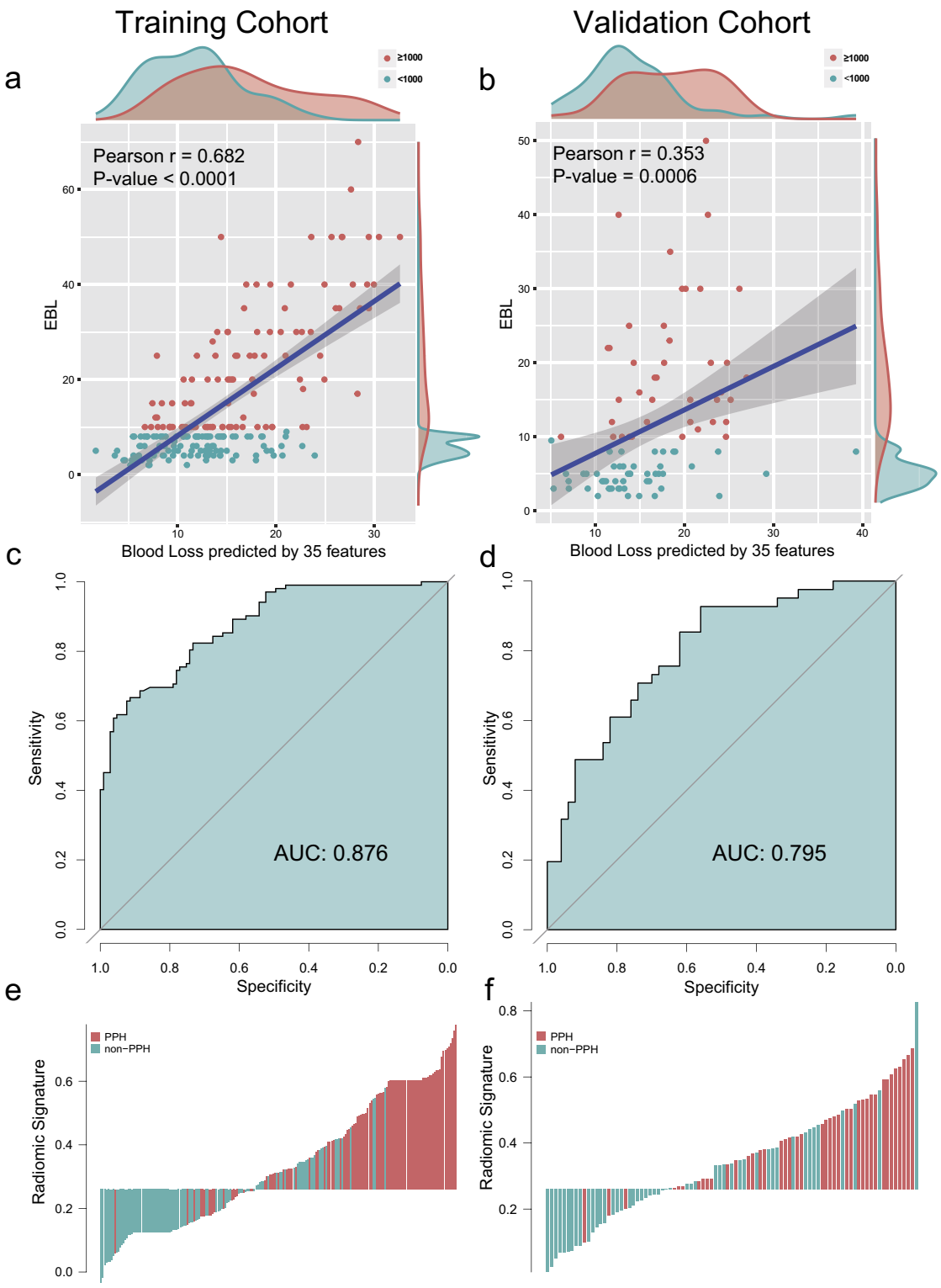

Fig. 4. Construction and evaluation of radiomic signature. (a,b) The correlation between the blood loss predicted by 35 radiomic features and estimated blood loss (EBL) of training cohort (a) and validation cohort (b). Each point represents a sample, with the red points for more than 1000 mL EBL and the blue points for less than 1000 mL EBL. The p-value of Pearson correlation analysis was < 0.0001 and 0.0006 respectively, indicating that the selected radiomic features were highly correlated with EBL. (c,d) The ROC curves of radiomic model, with an AUC of 0.876 (95% CI, 0.832–0.820) in the training cohort and 0.795 (95% CI, 0.705–0.885) in the validation cohort. (e,f) The radiomic signature histogram of training and validation cohort. The sample with postpartum hemorrhage (PPH) was indicated by red bar, and the sample without PPH was indicated by blue bar. The y-axis demonstrated the value of radiomic score. AUC: area under receiver operating characteristic curve.

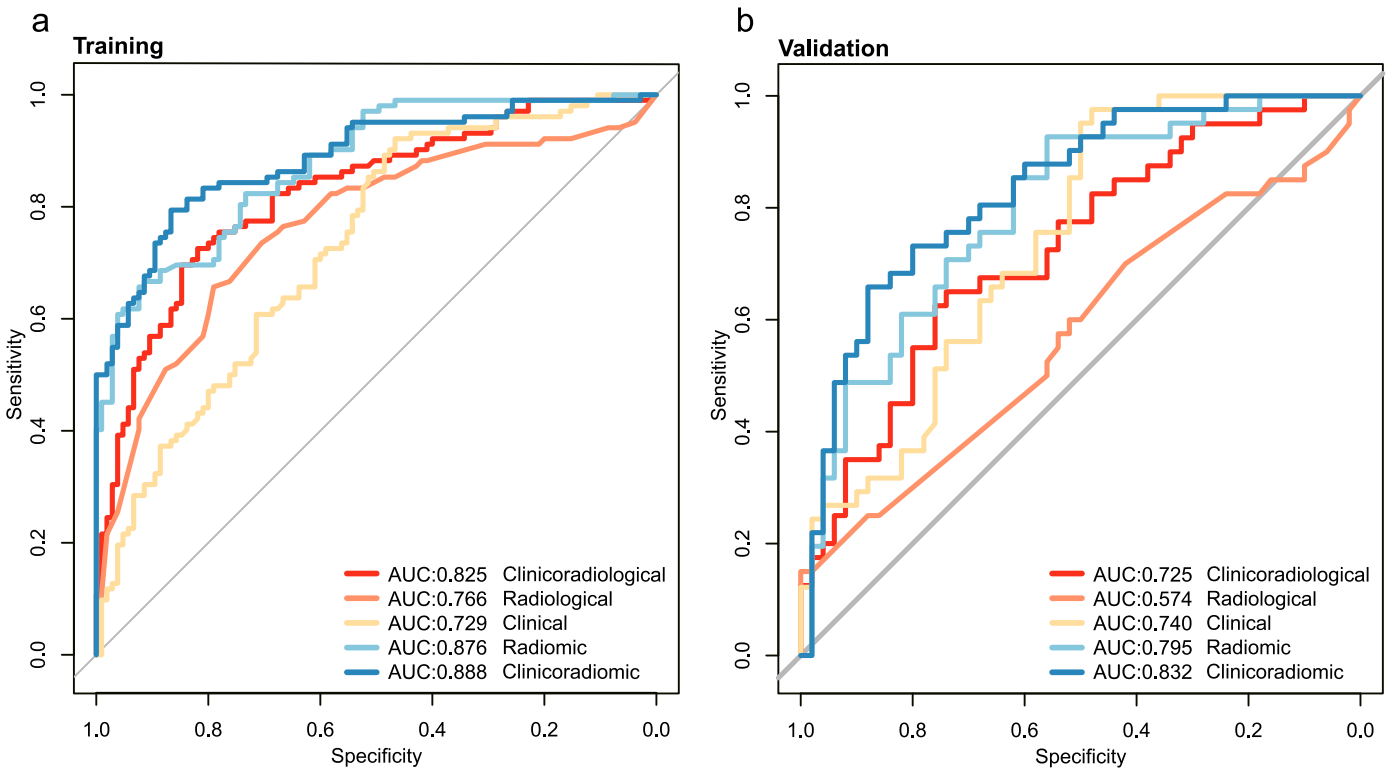

Fig. 5. Comparison of ROC curves of different models. (a) and (b) are ROC curves of the models in training and validation cohort. Among the five models, the clinicoradiomic model resulted in best performance, with an AUC of 0.888 in the training cohort and an AUC of 0.832 in the validation cohort.

Table 2
Performance of models for PPH prediction.

Cohort	Model	AUC	ACC (%)	SEN (%)	SPE (%)
Training Cohort	Clinical	0.729(0.660–0.796)	65.2(58.7–71.7)	63.7(54.2–73.0)	66.7(57.7–75.7)
	Radiological	0.766(0.699–0.833)	72.5(66.4–78.5)	65.7(56.4–74.9)	79.0(71.2–86.8)
	Radiomics	0.876(0.832–0.920)	74.4(68.6–80.2)	89.2(83.2–95.3)	60.0(50.6–69.2)
	Clinicoradiological	0.825(0.768–0.882)	76.3(70.5–82.2)	72.5(63.9–81.2)	80.0(72.4–87.5)
	Clinicoradiomics	0.888(0.844–0.933)	72.9(66.9–79.1)	91.2(85.8–96.7)	55.2(45.7–64.9)
Validation Cohort	Clinical	0.740(0.629–0.848)	62.6(52.3–72.7)	56.1(40.3–71.6)	68.0(54.4–81.3)
	Radiological	0.574(0.462–0.694)	54.9(44.7–65.5)	58.5(43.9–73.7)	52.0(37.9–66.3)
	Radiomics	0.795(0.705–0.885)	62.6(52.8–72.2)	92.7(84.8–100)	38.0(24.2–51.3)
	Clinicoradiological	0.725(0.618–0.832)	68.1(58.6–77.7)	63.4(48.4–78.7)	72.0(59.8–84.1)
	Clinicoradiomics	0.832(0.746–0.913)	68.1(58.6–77.5)	97.6(92.7–100)	44.0(30.2–57.5)

Abbreviations: PPH: Postpartum Haemorrhage.

Table 3
Performance of the radiomic nomogram for PPH prediction in pregnancies with and without PP.

Cohort	Subgroup	AUC	ACC (%)	SEN (%)	SPE (%)
Training	With PP	0.867(0.813–0.921)	71.0(64.2–77.9)	90.8(84.8–96.7)	50.0(39.1–61.2)
	Without PP	0.983(0.949–1.000)	84.2(72.7–95.3)	100(100–100)	73.9(55.9–91.2)
Validation	With PP	0.815(0.718–0.913)	67.9(57.3–78.4)	97.2(91.9–100)	42.9(27.9–57.8)
	Without PP	0.832(0.748–0.912)	68.1(58.7–77.4)	97.6(92.8–100)	44.0(30.3–57.4)

Abbreviations: PPH: Postpartum Haemorrhage; PP: Placenta Previa.

3.4. Clinical application of the clinicoradiomic model

The radiomic nomogram was defined based on the clinicoradiomic model, which showed the best discrimination ability among five models.

The calibration curve together with the H-L test was used to estimate the consistency between the probability of PPH predicted by the clinicoradiomic model and actual outcomes. As shown in Fig. 6b and c, the predicted probability of PPH is consistent with the actual PPH outcomes both in training and validation cohorts, with the p-value of 0.181 and 0.165, respectively.

The decision curve evaluated the performance for the clinicoradiomic model in terms of clinical application, hence, reflecting its clinical usefulness. In the DCA, the clinicoradiomic offered a net benefit over the treat-all-patients scheme or the treat-none scheme at a threshold probability >12% (Fig. 6d and e), which indicated that the clinicoradiomic was clinically useful.

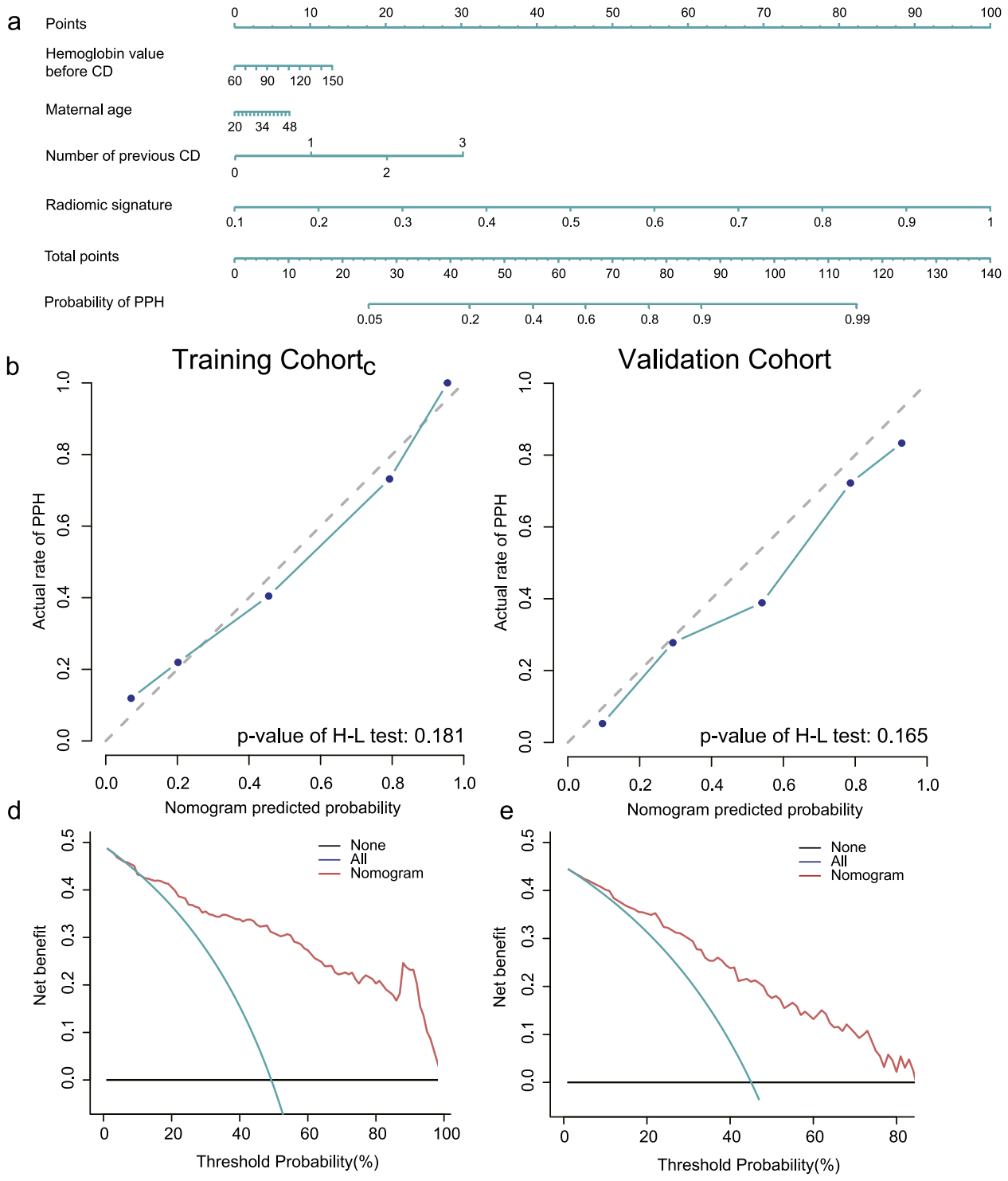

Fig. 6. The establishment and performance of the clinicoradiomic model. (a) The developed nomogram based on clinicoradiomicmodel. (b,c) Calibration curves of the clinicoradiomic model generated from the training and validation cohorts. The goodness of fits of predicted probability from the clinicoradiomic model with the actual outcomes of postpartum haemorrhage (PPH) was assessed. The x-axis represented the probability of PPH calculated by the clinicoradiomic model while the y-axis represented the actual rate of PPH. Diagonal dotted line represented a perfect estimation by an ideal model, in which the estimated outcome perfectly corresponded to the actual outcome. Solid line represented performance of the clinicoradiomic model, a closer alignment of which with the diagonal dotted line represented a better estimation. The p-value of H-L test was 0.181 and 0.165 respectively. (d,e) Decision curve analysis for the clinicoradiomic model. The x-axis showed the threshold probability and y-axis measured the net benefit. The red line represents the clinicoradiomic model. The blue line represented the assumption that all patients were PPH while the black line represented the assumption that no patients were PPH.

4. Discussion

This is the first large scale study to date to build a clinicoradiomic model to predict the risk of PPH in pregnant women antepartum based on placental radiomic features on T2WI . The performance of this model was validated in an external validation cohort with respect to discrimination, calibration curve and clinical application. Thirty-five radiomic features showed strong correlation with EBL, and were stable across multiple centers. The clinicoradiomic model combining both clinical factors and radiomic signature can identify more than 91% PPH and can be applied not only in pregnancies with PP, but also pregnancies without PP.

Nowadays the optimal management of PAS disorders remains undefined. Hysterectomy is recommended for patients with abnormally invasive placenta by the majority of members of the Society for Maternal-Fetal Medicine (SMFM) [26]. Three out of 207 pregnancies in the training cohort (1.45%) and 3 out of 91 pregnancies in the validation cohort (3.30%) underwent hysterectomy, which has the advantage of reducing the immediate risks of major haemorrhage associated with PAS disorders. For the intra-surgical diagnosis of PAS and preserving the uterus and fertility ability, attempted manual removal of the placenta was firstly employed for most pregnancies in the two hospitals of our study, which tend to result in massive obstetric haemorrhage. However, the correlation of EBL with clinical diagnosis of PAS disorders is significant in the training cohort while not in the validation cohort, as shown in Table S4. This is consistent with previous studies [27]. The contribution of PAS to the increase of PPH remains controversial. Mehrabadi A found that increases in placenta accrete cannot explain the recent increases in PPH, but contribute substantially to the proportion of PPH with hysterectomy [27]. Some cases of PAS underwent manual removal of placenta during CD did not submit pathological specimens, meanwhile, diagnosis of PAS requires an ideal textbook image of villi sitting atop muscle, which is hard to identify for patients without hysterectomy, and thus, cases with obvious gross invasion and without pathological diagnostic requirement of PAS frequently existed [28].

Recently several studies tried to build models to predict PPH, blood transfusion or severe complications based on clinical factors and ultrasound features of placenta [23,29–31]. All the pregnancies enrolled in these studies presented with PP. Although endpoints differed among these studies, the models showed promising results in predicting PPH. Clinical factors including patients' status and obstetrical histories were easy to identify, whereas the ultrasound features for these models including lacunae in placenta and uteroplacental hypervascularity were prone to be influenced by the experience of ultrasound doctors and differed among hospitals. Therefore, the performance of these models depends on situations. MRI provides more comprehensive evaluation of placenta compared with ultrasound. Radiomics quantifies placental heterogeneity thoroughly with various output features [32,33]. Our present study built the clinicoradiomic model by utilizing prenatal clinical factors and radiomic features of placenta on Sagittal T2WI for patients suspected with PAS disorders who underwent placental MRI. The clinicoradiomic model is not only applicable to pregnancies with PP, but also without PP. The PAS diagnosis based on ultrasound and MRI was not included in the model in order to avoid the subjective bias from the experience of doctors. Romeo V et al. found machine learning analysis of texture features of placenta on T2WI could identify PAS in patients with PP [18]. However, the region-of-interest based features might not reflect the heterogeneity of placenta. The delineation including not only the placenta, but also the subplacental tissue and the cervix for patients with PP ensured that the heterogeneity and surrounding circumstances completely assessed.

Not only for ultrasound, but also for MRI, the interobserver reliability for image features indicating PAS showed great variability when qualitatively evaluated [22], with kappa value of 0.24 for myometrial thinning and 0.85 for placental protrusion into internal os [34]. The great difference for the MRI features suggesting PAS between the training and validation cohorts in our study also illustrated the unreliability of image interpreting among different situations and radiologists. Thus quantitative assessment of images is needed for objective evaluation. Thirty-five radiomic features that showed strong correlation with EBL in both centers were enrolled in the radiomic and clinicoradiomic model. Although it is hard to interpret the specific underlying meaning of these radiomic features [35,36], the good performance of the model in the training and validation cohorts, in the subgroup with or without PP suggests that radiomics analysis is a useful and stable tool for EBL and PPH prediction. The stable performance in different centers also highlights that radiomics analysis can overcome data differences between multiple centers.

There were several limitations in our study. First, although efforts have been made to improve the accuracy of quantification of EBL, there was no recommended or preferred method from the guidelines, except either using a visible estimate or through the use of blood collection drapes, which showed unreliability among surgeons and institutions. However, EBL is still used to initiate levels of treatment in RCOG guidelines [37]. Second, the optimal timing of placental MRI and abnormal placentation detectable has not been clearly established in the literature [38]. Horowitz JM reported that placental MRI at 32–36 weeks showed best discriminative ability for PAS interpretation [39]. Whereas the 24–30 weeks of gestation were recommended as optimal time for MRI assessment of placenta accrete [40]. The gestation age when performing placental MRI in our study ranged from 27 to 41 weeks. Considering that, we also did not take the time interval between the MRI examination and CD into account. A future study with larger scale samples confined to specific gestational age would probably have better performance for PPH prediction. Third, the pathological diagnosis of PAS disorders was lacking in our study since not all of them underwent histological placental evaluation. Fourth, patients with twin or multiple pregnancies were not included in our study, thus the prediction model is not practical for these patients. Fifth, MRI is not as widely used for clinical use in pregnant women as ultrasound. Unlike previous models based on ultrasound features, the radiomic nomogram we built is limited to patients who underwent MRI. However, people seeking MRI are usually high risk with PP or suspected PAS, who will definitely benefit from the antepartum prediction of PPH with the radiomic nomogram we built.

5. Conclusion

Identification of pregnancies with postpartum haemorrhage (PPH) antenatally rather than intrapartum would aid delivery planning, facilitate transfusion requirements and decrease maternal complications. By radiomic analysis, thirty-five radiomic features showed strong correlation with EBL, which remained stable across multiple centers. The clinicoradiomic model incorporating both prenatal clinical factors and radiomic features of placenta on T2WI showed great performance in predicting PPH. The predictive model can identify severe PPH with high sensitivity and can be applied in patients with and without PP.

Declaration of Competing Interest

The authors declare no conflicts of interest.

Acknowledgments

We would like to thank Yan Wang, Ligang Shi, Yahui Xu (all from Henan Provincial People's Hospital) for the radiological image interpretation, pathological and obstetrical analyses.

Funding Sources

This study has received funding from National Key Research and Development Plan of China under Grant (2016YFA0100900, 2016YFA0100902, 2017YFA0205200, 2017YFE0103600), National Natural Science Foundation of China (81922040, 81772012, 81720108021), Beijing Natural Science Foundation (7182109), Key Project of Henan Province Medical Science and Technology Project (2018020422); Henan Key Scientific and Technological Research Project (192102310360), the Youth Innovation Promotion Association CAS (2019136). The funders had no role in study design, data collection, data analysis, interpretation orwriting of the report.

Supplementary materials

Supplementary material associated with this article can be found in the online version at doi:10.1016/j.ebiom.2019.11.010.

References

[1] Green L, Knight M, Seeney FM, Hopkinson C, Collins PW, Collis RE, et al. The epidemiology and outcomes of women with postpartum haemorrhage requiring massive transfusion with eight or more units of red cells: a national cross-sectional study. BJOG 2016;123(13):2164–70.

[2] Gatta LA, Lockhart EL, James AH. Blood products in the management of abnormal placentation. Clin Obstet Gynecol 2018;61(4):828–40.

[3] Fitzpatrick KE, Sellers S, Spark P, Kurinczuk JJ, Brocklehurst P, Knight M. The management and outcomes of placenta accreta, increta, and percreta in the UK: a population-based descriptive study. BJOG 2014;121(1):62–71.

[4] Shamshirsaz AA, Fox KA, Salmanian B, Diaz-Arrastia CR, Lee W, Baker BW, et al. Maternal morbidity in patients with morbidly adherent placenta treated with and without a standardized multidisciplinary approach. Am J Obstet Gynecol 2015;212(2) 218 e1-9.

[5] Morlando M, Sarno L, Napolitano R, Capone A, Tessitore G, Maruotti GM, et al. Placenta accreta: incidence and risk factors in an area with a particularly high rate of cesarean section. Acta Obstet Gynecol Scand 2013;92(4):457–60.

[6] Jauniaux E, Chantraine F, Silver RM, Langhoff-Roos J. FIGO consensus guidelines on placenta accreta spectrum disorders: epidemiology. Int J Gynaecol Obstet 2018;140(3):265–73.

[7] Sentilhes L, Kayem G, Chandraharan E, Palacios-Jaraquemada J, Jauniaux E. FIGO consensus guidelines on placenta accreta spectrum disorders: conservative management. Int J Gynaecol Obstet 2018;140(3):291–8.

[8] Jauniaux E, Collins S, Burton GJ. Placenta accreta spectrum: pathophysiology and evidence-based anatomy for prenatal ultrasound imaging. Am J Obstet Gynecol 2018;218(1):75–87.

[9] Balcacer P, Pahade J, Spektor M, Staib L, Copel JA, McCarthy S. Magnetic resonance imaging and sonography in the diagnosis of placental invasion. J Ultrasound Med 2016;35(7):1445–56.

[10] Meng X, Xie L, Song W. Comparing the diagnostic value of ultrasound and magnetic resonance imaging for placenta accreta: a systematic review and meta-analysis. Ultrasound Med Biol 2013;39(11):1958–65.

[11] D'Antonio F, Iacovella C, Palacios-Jaraquemada J, Bruno CH, Manzoli L, Bhide A. Prenatal identification of invasive placentation using magnetic resonance imaging: systematic review and meta-analysis. Ultrasound Obstet Gynecol 2014;44(1):8–16.

[12] Einerson BD, Rodriguez CE, Kennedy AM, Woodward PJ, Donnelly MA, Silver RM. Magnetic resonance imaging is often misleading when used as an adjunct to ultrasound in the management of placenta accreta spectrum disorders. Am J Obstet Gynecol 2018;218(6) 618 e1- e7.

[13] Zaghal AA, Hussain HK, Berjawi GA. MRI evaluation of the placenta from normal variants to abnormalities of implantation and malignancies. J Magn Reson Imaging 2019 https://doi.org/10.1002/jmri.26764.

[14] Liu Z, Zhang XY, Shi YJ, Wang L, Zhu HT, Tang Z, et al. Radiomics analysis for evaluation of pathological complete response to neoadjuvant chemoradiotherapy in locally advanced rectal cancer. Clin Cancer Res 2017;23(23):7253–62.

[15] Liu Z, Wang S, Dong D, Wei J, Fang C, Zhou X, et al. The applications of radiomics in precision diagnosis and treatment of oncology: opportunities and challenges. Theranostics 2019;9(5):1303–22.

[16] Wu Q, Wang S, Chen X, Wang Y, Dong L, Liu Z, et al. Radiomics analysis of magnetic resonance imaging improves diagnostic performance of lymph node metastasis in patients with cervical cancer. Radiother Oncol 2019;138:141–8.

[17] Siauve N. How and why should the radiologist look at the placenta? Eur Radiol 2019;29(11):6149–51.

[18] Romeo V, Ricciardi C, Cuocolo R, Stanzione A, Verde F, Sarno L, et al. Machine learning analysis of MRI-derived texture features to predict placenta accreta spectrum in patients with placenta previa. Magn Reson Imaging 2019 https://doi.org/10.1016/j.mri.2019.05.017.

[19] Do QN, Lewis MA, Xi Y, Madhuranthakam AJ, Happe SK, Dashe JS, et al. MRI of the placenta accreta spectrum (PAS) disorder: radiomics analysis correlates with surgical and pathological outcome. J Magn Reson Imaging 2019 https://doi.org/10.1002/jmri.26883.

[20] Chen E, Mar WA, Horowitz JM, Allen A, Jha P, Cantrell DR, et al. Texture analysis of placental MRI: can it aid in the prenatal diagnosis of placenta accreta spectrum? Abdominal Radiology 2019;44(9):3175–84.

[21] Bourgioti C, Zafeiropoulou K, Fotopoulos S, Nikolaidou ME, Antoniou A, Tzavara C, et al. MRI features predictive of invasive placenta with extrauterine spread in high-risk gravid patients: a prospective evaluation. AJR Am J Roentgenol 2018;211(3):701–11.

[22] Bour L, Place V, Bendavid S, Fargeaudou Y, Portal JJ, Ricbourg A, et al. Suspected invasive placenta: evaluation with magnetic resonance imaging. Eur Radiol 2014;24(12):3150–60.

[23] Lee JY, Ahn EH, Kang S, Moon MJ, Jung SH, Chang SW, et al. Scoring model to predict massive post-partum bleeding in pregnancies with placenta previa: a retrospective cohort study. J Obstet Gynaecol Res 2018;44(1):54–60.

[24] Bertucci E, Sileo FG, Grandi G, Fenu V, Cani C, Mancini L, et al. The jellyfish sign: a new sonographic cervical marker to predict maternal morbidity in abnormally invasive placenta previa. Ultraschall Med 2019;40(1):40–6.

[25] Miller TD, Askew JW. Net reclassification improvement and integrated discrimination improvement: new standards for evaluating the incremental value of stress imaging for risk assessment. Circ Cardiovasc Imaging 2013;6(4):496–8.

[26] Allen L, Jauniaux E, Hobson S, Papillon-Smith J, Belfort MA. FIGO consensus guidelines on placenta accreta spectrum disorders: nonconservative surgical management. Int J Gynaecol Obstet 2018;140(3):281–90.

[27] Mehrabadi A, Hutcheon JA, Liu S, Bartholomew S, Kramer MS, Liston RM, et al. Contribution of placenta accreta to the incidence of postpartum hemorrhage and severe postpartum hemorrhage. Obstet Gynecol 2015;125(4):814–21.

[28] Dannheim K, Shainker SA, Hecht JL. Hysterectomy for placenta accreta; methods for gross and microscopic pathology examination. Arch Gynecol Obstet 2016;293(5):951–8.

[29] Baba Y, Ohkuchi A, Usui R, Suzuki H, Kuwata T, Matsubara S. Calculating probability of requiring allogeneic blood transfusion using three preoperative risk factors on cesarean section for placenta previa. Arch Gynecol Obstet 2015;291(2):281–5.

[30] Yoon SY, You JY, Choi SJ, Oh SY, Kim JH, Roh CR. A combined ultrasound and clinical scoring model for the prediction of peripartum complications in pregnancies complicated by placenta previa. Eur J Obstet Gynecol Reprod Biol 2014;180:111–5.

[31] Kim JW, Lee YK, Chin JH, Kim SO, Lee MY, Won HS, et al. Development of a scoring system to predict massive postpartum transfusion in placenta previa totalis. J Anesth 2017;31(4):593–600.

[32] Sun C, Tian X, Liu Z, Li W, Li P, Chen J, et al. Radiomic analysis for pretreatment prediction of response to neoadjuvant chemotherapy in locally advanced cervical cancer: a multicentre study. EBioMedicine 2019;46:160–9.

[33] Liu Z, Wang Y, Liu X, Du Y, Tang Z, Wang K, et al. Radiomics analysis allows for precise prediction of epilepsy in patients with low-grade gliomas. Neuroimage Clin 2018;19:271–8.

[34] Ueno Y, Kitajima K, Kawakami F, Maeda T, Suenaga Y, Takahashi S, et al. Novel MRI finding for diagnosis of invasive placenta praevia: evaluation of findings for 65 patients using clinical and histopathological correlations. Eur Radiol 2014;24(4):881–8.

[35] Wang S, Liu Z, Rong Y, Zhou B, Bai Y, Wei W, et al. Deep learning provides a new computed tomography-based prognostic biomarker for recurrence prediction in high-grade serous ovarian cancer. Radiother Oncol 2019;132:171–7.

[36] Zhou X, Yi Y, Liu Z, Cao W, Lai B, Sun K, et al. Radiomics-Based pretherapeutic prediction of non-response to neoadjuvant therapy in locally advanced rectal cancer. Ann Surg Oncol 2019;26(6):1676–84.

[37] Dahlke JD, Mendez-Figueroa H, Maggio L, Hauspurg AK, Sperling JD, Chauhan SP, et al. Prevention and management of postpartum hemorrhage: a comparison of 4 national guidelines. Am J Obstet Gynecol 2015;213(1) 76 e1- e10.

[38] Leyendecker JR, DuBose M, Hosseinzadeh K, Stone R, Gianini J, Childs DD, et al. MRI of pregnancy-related issues: abnormal placentation. AJR Am J Roentgenol 2012;198(2):311–20.

[39] Horowitz JM, Berggruen S, McCarthy RJ, Chen MJ, Hammond C, Trinh A, et al. When timing is everything: are placental MRI examinations performed before 24 weeks' gestational age reliable? AJR Am J Roentgenol 2015;205(3):685–92.

[40] Kilcoyne A, Shenoy-Bhangle AS, Roberts DJ, Sisodia RC, Gervais DA, Lee SI. MRI of placenta accreta, placenta increta, and placenta percreta: pearls and pitfalls. AJR Am J Roentgenol 2017;208(1):214–21.